



Article

Pediatric and Adolescent Seizure Detection: A Machine Learning Approach Exploring the Influence of Age and Sex in Electroencephalogram Analysis [†]

Lan Wei and Catherine Mooney *

FutureNeuro SFI Research Centre, School of Computer Science, University College Dublin, D02 YN77 Dublin, Ireland; lan.wei@ucd.ie

* Correspondence: catherine.mooney@ucd.ie

[†] This paper is an extended version of our paper published in Wei, L.; Mooney, C. Investigating the Need for Pediatric-Specific Machine Learning Approaches for Seizure Detection in EEG. In Proceedings of the 2023 11th International Conference on Bioinformatics and Computational Biology (ICBCB), Hangzhou, China, 21–23 April 2023; IEEE: New York, NY, USA, 2023, pp. 57–63.

Abstract: Background: Epilepsy, a prevalent neurological disorder characterized by recurrent seizures affecting an estimated 70 million people worldwide, poses a significant diagnostic challenge. EEG serves as an important tool in identifying these seizures, but the manual examination of EEGs by experts is time-consuming. To expedite this process, automated seizure detection methods have emerged as powerful aids for expert EEG analysis. It is worth noting that while such methods are well-established for adult EEGs, they have been underdeveloped for pediatric and adolescent EEGs. This study sought to address this gap by devising an automatic seizure detection system tailored for pediatric and adolescent EEG data. Methods: Leveraging publicly available datasets, the TUH pediatric and adolescent EEG and CHB-MIT EEG datasets, the machine learning-based models were constructed. The TUH pediatric and adolescent EEG dataset was divided into training (n = 118), validation (n = 19), and testing (n = 37) subsets, with special attention to ensure a clear demarcation between the individuals in the training and test sets to preserve the test set's independence. The CHB-MIT EEG dataset was used as an external test set. Age and sex were incorporated as features in the models to investigate their potential influence on seizure detection. Results: By leveraging 20 features extracted from both time and frequency domains, along with age as an additional feature, the method achieved an accuracy of 98.95% on the TUH test set and 64.82% on the CHB-MIT external test set. Our investigation revealed that age is a crucial factor for accurate seizure detection in pediatric and adolescent EEGs. Conclusion: The outcomes of this study hold substantial promise in supporting researchers and clinicians engaged in the automated analysis of seizures in pediatric and adolescent EEGs.



Citation: Wei, L.; Mooney, C. Pediatric and Adolescent Seizure Detection: A Machine Learning Approach Exploring the Influence of Age and Sex in Electroencephalogram Analysis. *BioMedInformatics* **2024**, *4*, 796–810. <https://doi.org/10.3390/biomedinformatics4010044>

Academic Editor: Alexandre G. De Brevenc

Received: 30 January 2024

Revised: 21 February 2024

Accepted: 5 March 2024

Published: 6 March 2024



Copyright: © 2024 by the authors. Licensee MDPI, Basel, Switzerland. This article is an open access article distributed under the terms and conditions of the Creative Commons Attribution (CC BY) license (<https://creativecommons.org/licenses/by/4.0/>).

Keywords: EEG; epilepsy; age; sex; children; pediatric and adolescent; seizures; seizure detection

1. Introduction

Epilepsy, a prevalent neurological disorder characterized by recurrent seizures that affect an estimated 70 million people worldwide, presents a substantial diagnostic challenge [1]. It is characterized by a persistent propensity to experience spontaneous epileptic seizures, resulting in diverse neurobiological, cognitive, and psychosocial consequences. In children, the causes and clinical manifestations of epilepsy encompass a wide spectrum [2].

The electroencephalogram (EEG) is an important clinical tool for diagnosing seizures and epilepsy [3]. Nonetheless, the manual identification of seizure events in EEG recordings is a labor-intensive process. Automatic seizure detection methods have emerged as powerful tools that can aid researchers in the analysis of seizures, garnering increasing attention in recent times.

There is considerable optimism surrounding the integration of artificial intelligence (AI) into healthcare, with the potential to significantly enhance various facets of the field, spanning from diagnosis to treatment. Rather than displacing healthcare professionals, AI is viewed as a complementary tool to augment and streamline their efforts. It can aid in a wide array of tasks, including administrative processes, clinical documentation, patient engagement, and specialized assistance [4]. The use of machine learning techniques [5–7] has facilitated advancements in medical diagnosis, prediction of future ailments or events, and enhancements in preventive care and treatment methodologies.

Several studies have introduced deep-learning-based seizure detection methods tailored for TUH EEGs. Golmohammadi et al. [8] employed Convolutional Neural Networks (CNN) and Long Short-Term Memory Networks (LSTM), achieving a sensitivity of 30% on the test set. Shah et al. [9] used a three-layer 2D CNN, achieving a sensitivity of 39.15%. Ziyabari et al. [10] combined CNN and Multilayer Perceptron techniques, resulting in a sensitivity of 31.58%. Additionally, Albaqami et al. [11] proposed a WaveNet–Long Short-Term Memory (LSTM) approach for the automatic detection of abnormal raw EEG data, achieving a classification accuracy of 88.76%. Although there has been substantial research in the development of seizure detection methods for adult EEGs [10,12,13], the field of pediatric and adolescent-based seizure detection methods remains relatively underdeveloped. Notably, EEG patterns have been observed to undergo changes with aging [14]. It is well-established that attempting to adapt adult-centric methodologies for use in pediatric and adolescent cases is not a viable approach [15]. Thus, there is an urgent demand for the development of seizure detection methods tailored specifically to the pediatric and adolescent population [15]. Furthermore, it is essential to investigate potential variations in age-related patterns in pediatric and adolescent EEG activity and determine how these variances might impact the ability to detect seizures in pediatric and adolescent EEG recordings.

Numerous studies have investigated age-related differences in EEG patterns [15–17]. Some researchers have observed that older adults exhibit greater activity in the higher frequency beta band compared to younger adults, particularly in baseline conditions that require no mental effort [18,19]. Additionally, certain studies [20] have indicated that older adults demonstrate lower percentages of theta and alpha activity and higher percentages of beta activity when performing mental arithmetic tasks, in contrast to their younger counterparts. However, conflicting findings have emerged from other investigations, with some reporting shifts in EEG frequency spectra toward lower frequencies with advancing age [21], while others have found no significant age-related differences at all [22]. Gasser et al. [23] analyzed typically developing children aged 6 to 17, revealing only a modest increase in EEG coherence with age.

In our earlier investigation [15], models were trained on adult EEG data from the TUH dataset and evaluated on the CHB-MIT EEG dataset. Unfortunately, this strategy yielded limited success, achieving only 10.5% accuracy and balanced accuracy of 50.8% on the CHB-MIT EEG dataset. Consequently, employing an adult-based seizure detection method proves unsuitable for children and adolescents. To address this limitation, there is a necessity to formulate a seizure detection method specifically tailored for pediatric and adolescent cases. Additionally, age should be considered as a feature in the development of automated seizure detection algorithms.

Reports on sex differences in the normal maturation of the EEG have yielded mixed results [24]. Previous research has identified EEG disparities between boys and girls that suggest earlier maturation in girls [25,26]. However, some studies have failed to detect EEG distinctions between male and female children [23,27]. In contrast, Matthis et al. [28] found that, at the age of six, girls exhibit relatively more theta and less alpha activity.

Previous research [16] also demonstrated statistically significant differences in relative theta and alpha activity between male and female children in EEGs. Therefore, it is pertinent to explore potential dissimilarities in EEG patterns between male and female children and

to investigate whether these disparities influence the detection of seizures in pediatric and adolescent EEGs.

Light Gradient Boosting Machine (LightGBM) represents a gradient boosting framework leveraging tree-based learning algorithms tailored for distributed and efficient training of extensive datasets. Recognized for its exceptional speed, efficiency, and scalability, LightGBM stands as a preferred solution for EEG analysis tasks [29–31]. In this study, LightGBM-based automatic seizure detection methods using the TUH pediatric and adolescent EEG recordings were developed. The patient data were meticulously partitioned into distinct training and testing sets to ensure no overlap, and the CHB-MIT EEG data were used as an external test set to assess the performance of the developed method. The method achieved 98.95% cross-subject accuracy (training and testing on different subjects) for the TUH pediatric and adolescent EEG dataset and 64.82% cross-database accuracy (training and testing on different databases) for the CHB-MIT EEGs. Furthermore, an investigation was conducted to determine whether age and sex influence the detection of seizures in pediatric and adolescent EEG data. The findings hold significant promise in providing valuable support to researchers and clinicians involved in the automated analysis of pediatric and adolescent EEGs for seizure detection.

2. Data

2.1. TUH EEG Dataset

The Department of Neurology at Temple University Hospital (TUH) hosts the largest accessible clinical EEG data repository globally [32]. The TUH EEG dataset includes focal non-specific seizures, generalized seizures, tonic-clonic seizures, and tonic seizures [33]. In this research, the TUH seizure corpus version 1.5.1 was employed to explore how age and sex impact seizure detection in pediatric and adolescent EEGs. EEG recordings from children and adolescents aged 1 to 20 (comprising 192 recordings) were specifically selected. EEG recordings that lacked age and sex information were excluded, resulting in the removal of eight recordings. Thus, the training dataset comprised 118 EEG recordings, the validation dataset included 29 EEG recordings, and an additional set of 37 pediatric and adolescent EEGs was reserved for independent testing.

2.2. CHB-MIT EEG Dataset

The CHB-MIT Scalp EEG Database is a publicly accessible EEG database that was compiled at the Children’s Hospital Boston (CHB) [34]. It encompasses data from 22 subjects, whose ages range from 1 to 22 years, primarily consisting of clonic, tonic, and atonic seizures. The pediatric and adolescent EEG recordings from the CHB-MIT database were used as an external, independent test set. Table 1 provides a comprehensive overview of the dataset used. Figure 1 presents the examples of seizure events in channel C3-P3 for both the TUH children and CHB-MIT datasets.

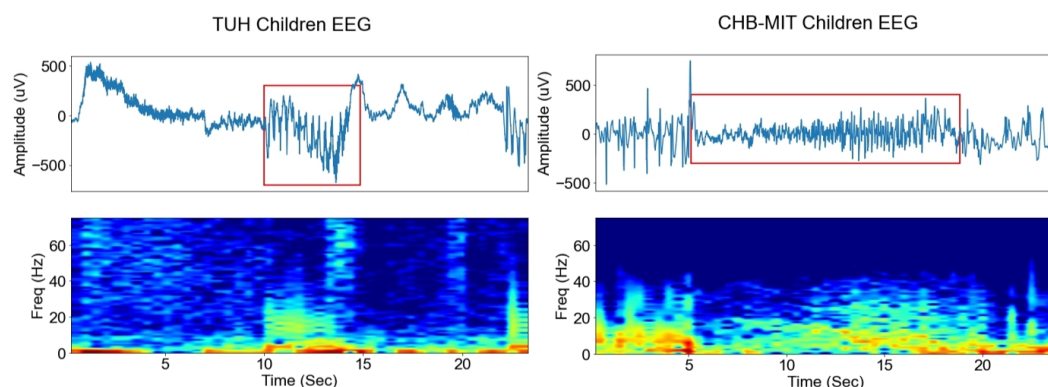


Figure 1. The figure illustrates examples of seizure events in channel C3-P3 for both the TUH children and CHB-MIT datasets. Each example consists of 24 s of EEG recordings along with their corresponding spectrograms. The signal in the red block indicates the occurrence of a seizure.

The flowchart presented in Figure 2 outlines the models developed within this study. The TUH pediatric and adolescent EEG dataset was partitioned, allocating 60% for training the model and 20% for validation. The remaining 20% of the TUH pediatric and adolescent EEG dataset, combined with the CHB-MIT EEG data, formed the independent test dataset to demonstrate the method’s stability. Within the training set, there were 58 female and 60 male subjects. Additionally, among these subjects, 56 had pediatric and adolescent EEG recordings for ages equal to or younger than 10 years old, while 62 subjects had pediatric and adolescent EEG recordings for ages older than 10 years old. The validation set comprised 12 females and 17 males. In total, 11 were children aged equal to or younger than 10 years old, and 18 were children older than 10 years old. The remaining 37 TUH pediatric EEGs were used for independent testing. This set included 21 females and 16 males, with 11 children aged equal to or younger than 10 years old and 26 children older than 10 years old. All available CHB-MIT EEG data were used for the external test dataset, totaling five males and 17 females. A total of 12 were children aged equal to or younger than 10 years old, and 10 were children older than 10 years old.

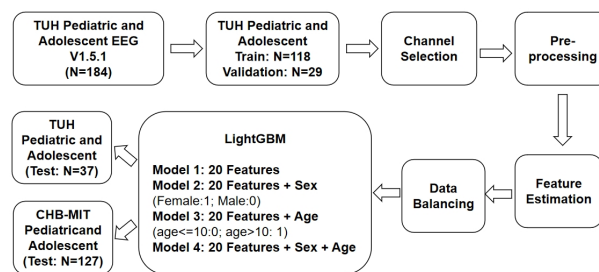


Figure 2. Overview of the seizure detection methods employing LightGBM. The algorithm was trained using TUH pediatric and adolescent EEGs. Subsequently, TUH pediatric and adolescent EEGs and CHB-MIT pediatric and adolescent EEGs were employed for the independent testing of these methods.

Table 1. Table displaying the duration of seizures and non-seizures within the EEG recordings from TUH and CHB-MIT used in this research.

	TUH EEG Files	CHB-MIT EEG Files
Total file number	184	127
Total seizure duration(s)	7602.0	11,117
Total non-seizure duration(s)	68,069.5	624,279.5
Patient number	184	22
Age range	1–20	1–22

3. Methodology

3.1. Channel Selection

Recording EEG signals is a highly intricate procedure that demands adaptation to the distinctive channel layouts associated with various EEG or clinical sites [35]. To ensure the applicability of this method to the CHB-MIT EEG dataset, a set of overlapping channels was opted for shared between the TUH EEG recordings and the CHB-MIT EEG dataset. The TUH EEG recordings lack temporal lines, and as a result, they do not include the FZ-CZ and CZ-PZ channels. As a result, the use of signals from the temporal lines to develop the model proved to be ineffective. Furthermore, to mitigate the risk of overfitting and to retain essential information, five channels from different brain regions were selected. These channels include FP1-F7, FP1-F3, P3-O1, C3-P3, and F3-C3.

3.2. Data Pre-Processing

The CHB-MIT EEG dataset was initially recorded at a sampling rate of 256 Hz, while the TUH EEG data encompassed various sampling frequencies—250 Hz, 256 Hz, 400 Hz,

and 1000 Hz. To maintain uniformity, the TUH EEG signals underwent consistent resampling to a rate of 256Hz. Moreover, a notch filter (60 Hz) was applied to eliminate powerline interference, and the DC offset was removed from the EEG data in both datasets. Furthermore, the EEG signals were segmented into 1 s epochs, each containing 256 data points, with a 0.5 s overlap. Each epoch corresponds to either a seizure event or a non-seizure event.

3.3. Feature Estimation

Features from both the time and frequency domains were calculated. Butterworth filters with a sixth order were employed to filter the signals within specific frequency bands of interest, including theta (4–8 Hz), alpha (8–13 Hz), beta (13–32 Hz), and gamma (>32 Hz). For the feature extraction process, 1 s epochs with a 0.5 s overlap were used, resulting in the estimation of 20 features for each channel. In the training set, data from five channels were used, leading to a total of 100 features. The features extracted from each channel are as follows:

Time domain features:

1. Mean value of the pre-processed absolute amplitude of EEG recordings;
2. Standard deviation of the pre-processed absolute amplitude of EEG recordings;
3. Skewness of the pre-processed absolute amplitude of EEG recordings;
4. Signal envelope of the pre-processed absolute amplitude of EEG recordings;
5. Kurtosis of the pre-processed absolute amplitude of EEG recordings;
6. Complexity of the pre-processed absolute amplitude of EEG recordings;
7. Mobility of the pre-processed absolute amplitude of EEG recordings;
8. Teager–Kaiser energy operator (TKEO) of the pre-processed absolute amplitude of EEG recordings;
9. Variance of the pre-processed absolute amplitude of EEG recordings;
10. Fractal dimension (FD) of the pre-processed absolute amplitude of EEG recordings.

Frequency domain features: Ten features were estimated as follows:

1. Relative band power of theta;
2. Absolute band power of theta;
3. Relative band power of alpha;
4. Absolute band power of alpha;
5. Relative band power of beta;
6. Absolute band power of beta;
7. Relative band power of gamma;
8. Absolute band power of gamma;
9. Absolute band power of the EEG amplitude;
10. Sum of relative band power of beta and gamma.

$$\text{TKEO}[n] = x[n]^2 - x[n-1]x[n+1] \quad (1)$$

$$\text{FD} = \frac{\log_{10}^n}{\log_{10}^n + \log_{10}^{n/(n+0.4\delta)}} \quad (2)$$

$$\text{Mobility} = \sqrt{\frac{\text{Var}(\dot{x})}{\text{Var}(x)}} \quad (3)$$

where

- n represents the number of samples within each epoch;
- δ signifies the number of sign changes in the signal derivative in that epoch;
- \dot{x} denotes the time derivative of the pre-processed EEG signal x ;
- $x[n]$ stands for the n^{th} sample, $x[n-1]$ refers to the $(n-1)^{\text{th}}$ sample and $x[n+1]$ indicates the $(n+1)^{\text{th}}$ sample of the pre-processed EEG signal within the epoch;
- $\text{Var}(x)$ represents the variance of x estimated for that epoch.

To explore the influence of age and sex on seizure detection in pediatric and adolescent EEG data, sex (male and female) and age group were introduced as additional features. Children were categorized into age groups, with one group comprising those older than 10 years and the other including those aged 10 years or younger.

3.4. Data Balancing

The total duration of seizure events is notably shorter in comparison to non-seizure events, as indicated in Table 1. This inherent class imbalance poses challenges for training machine learning algorithms. Consequently, the Synthetic Minority Over-sampling Technique (SMOTE) [36] was employed to rebalance the data within the training set.

3.5. Classification Algorithms

LightGBM [37] has been used in diverse data mining tasks, encompassing classification, regression, and ranking [37]. The LightGBM algorithm leverages two innovative techniques: gradient-based one-sided sampling and exclusive feature bundling. LightGBM's superiority lies in its efficient handling of large-scale datasets, optimized training speed, and exceptional predictive accuracy [37]. The algorithm's optimization objectives and tree-based learning architecture enabled it to capture intricate patterns within the EEG data, resulting in heightened performance in seizure detection tasks. The interpretability of feature importance provided by LightGBM facilitated a deeper understanding of the significance of different features, guiding the development of more refined and effective seizure detection models [38].

To explore the influence of age and sex on seizure detection in pediatric and adolescent EEG, four distinct models were built using LightGBM. We experimented with a random forest algorithm, decision tree and Extreme Gradient Boosting (XGBoost); however, the performance did not match the GBM (results not shown). All models used LightGBM with the same parameters. Two parameters were optimized: *n*-estimators (representing the number of boosted trees to fit) and learning rate (pertaining to the boosting learning rate). This optimization process relied on the performance assessment of the validation set aimed at enhancing the method's efficacy in detecting seizures in the TUH pediatric EEG recordings. Tests across a range of values were conducted, examining *n*-estimators from 10 to 500 and learning rates from 0.001 to 0.1. The optimal performance on the validation set was attained when *n*-estimators equaled 50 and the learning rate was set to 0.1.

The distinction among models lies in the variation of input features, enabling a comprehensive evaluation of the impact of different features on seizure detection efficacy. Model 1 used 20 features sourced from both time and frequency domains as the input for the LightGBM algorithm. In Model 2, the inclusion of sex as an additional feature augmented Model 1. Similarly, Model 3 expanded upon Model 1 by integrating age as an additional feature. Lastly, Model 4 enhanced the feature set of Model 1 by incorporating both sex and age as supplementary features. The methods employed for model development are elaborated below. The illustration in Figure 3 depicts the intricacies of the developed models.

- Model 1 was trained and evaluated using the 20 features derived from both time and frequency domains as described in Section 3.3.
- Model 2 was trained and tested on the same 20 features (Section 3.3). However, it incorporated an additional feature, namely sex (male and female, where 0 denotes female and 1 denotes male), resulting in a total of 21 features.
- Model 3 was trained and tested using the original 20 features (Section 3.3) and added age group (where 0 represents children aged 10 or younger, and 1 represents children older than 10) as an additional feature, this totaled 21 features in the model.
- Model 4 was trained and tested on the same 20 features (Section 3.3), but integrated both sex and age group as additional features, thus employing a total of 22 features in its development.

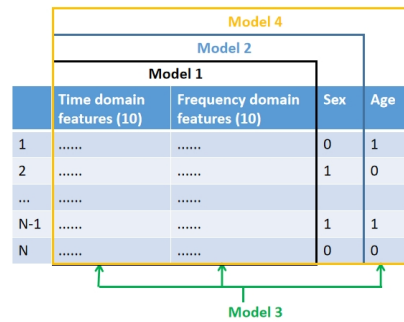


Figure 3. The techniques used in model development encompass various approaches. Model 1 utilizes features from both time and frequency domains. Model 2 incorporates gender as a feature (where 0 denotes female and 1 denotes male). Model 3 includes age groups as a feature (where 0 represents children aged 10 or younger, and 1 represents children older than 10). Model 4 integrates both gender and age groups as features.

3.6. Performance Evaluation

As seizure detection involves binary classification, the methods’ performance was assessed using sensitivity (*Sens*), specificity (*Spec*), accuracy (*Acc*) and balanced accuracy (*BAcc*).

$$\begin{aligned}
 Sens &= \frac{TP}{TP + FN} \\
 Spec &= \frac{TN}{TN + FP} \\
 Acc &= \frac{TP + TN}{TP + TN + FP + FN} \\
 BAcc &= \frac{Sens + Spec}{2}
 \end{aligned}
 \tag{4}$$

where:

- True Positives (*TP*): the number of seizures correctly predicted as seizures.
- False Positives (*FP*): the number of non-seizures incorrectly predicted as seizures.
- True Negatives (*TN*): the number of non-seizures correctly predicted as non-seizures.
- False Negatives (*FN*): the number of seizures incorrectly predicted as non-seizures.

4. Results

4.1. Feature Importance

Figure 4 shows the LightGBM-based feature importance plot (top 10) in the training set. These top 10 features are (1) C3–P3 TKEO, (2) FP1–F3 TKEO, (3) FP1–F7 TKEO, (4) P3–O1 TKEO, (5) FP1–F7 FD, (6) age group, (7) FP1–F3 variance (*var*), (8) F3–C3 signal envelop, (9) FP1–F7 signal envelop, and (10) FP1–F3 TKEO. It is clear to see that the TKEO is an important feature in identifying seizure and non-seizure events.

4.2. Feature Analysis

Figure 5 and Table 2 illustrate a comparison of TKEO between seizure events and non-seizure events across five selected channels on TUH pediatric and adolescent EEG and CHB-MIT pediatric and adolescent EEG. Notably, significant distinctions in TKEO are evident between seizure and non-seizure events across various channels.

Figure 6 presents a comparison of the mean amplitude between seizure events and non-seizure events, with a focus on males and females, across five specific channels in the TUH pediatric and adolescent EEG and CHB-MIT pediatric and adolescent EEG datasets.

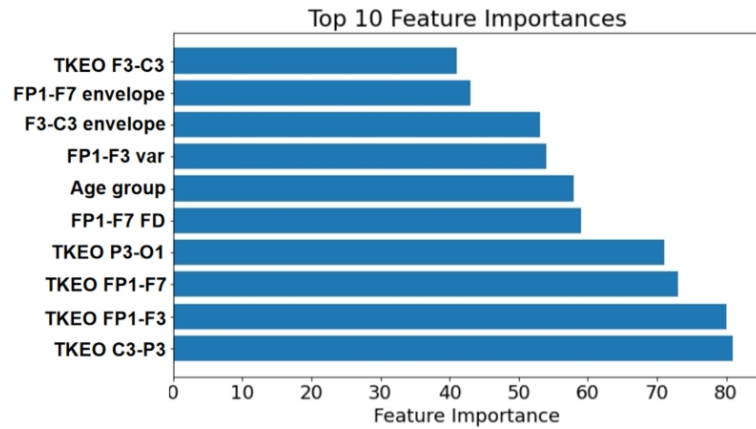


Figure 4. The ten most significant features within the training set.

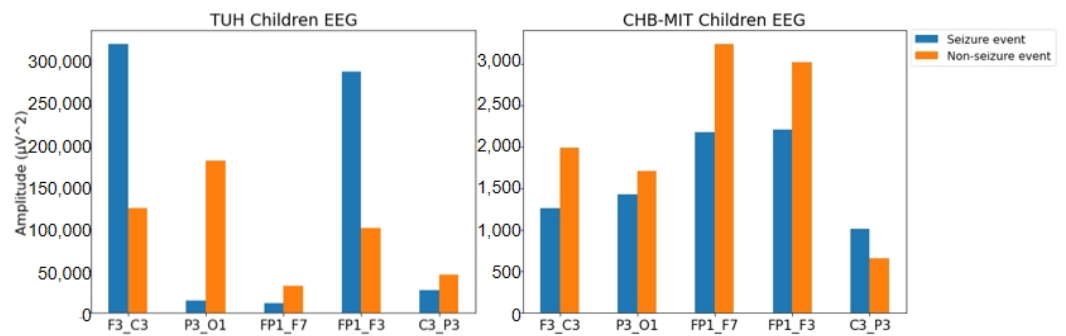


Figure 5. Comparison of TKEO between seizure events and non-seizure events across five selected channels on TUH pediatric and adolescent EEG and CHB-MIT pediatric and adolescent EEG.

Table 2. Comparison of TKEO between seizure events and non-seizure events across five selected channels on TUH pediatric and adolescent EEG and CHB-MIT pediatric and adolescent EEG.

	(μV^2)	F3-C3	P3-O1	FP1-F7	FP1-F3	C3-P3
TUH	Seizure	325,324.41	14,638.42	10,969.92	292,015.61	26,648.72
	Non-seizure	125,824.93	183,742.85	31,594.45	102,562.60	45,582.13
CHB-MIT	Seizure	1255.52	1422.89	2180.98	2209.52	1004.26
	Non-seizure	1991.31	1707.90	3242.40	3021.55	657.07

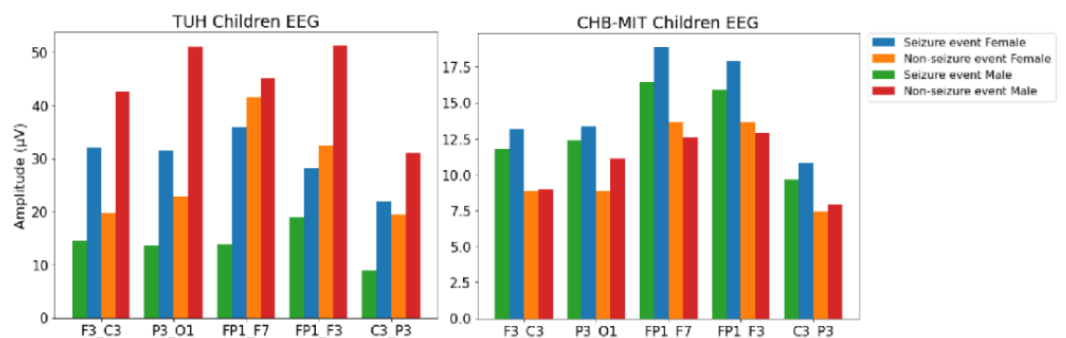


Figure 6. Comparison of mean amplitude between seizure events and non-seizure events for males and females across five selected channels on the TUH pediatric and adolescent EEG and CHB-MIT pediatric and adolescent EEG.

Figure 7 displays a comparison of mean amplitude between seizure events and non-seizure events in children aged over 10 and those aged 10 or younger, considering five selected channels in the TUH pediatric and adolescent EEG and CHB-MIT pediatric and adolescent EEG datasets.

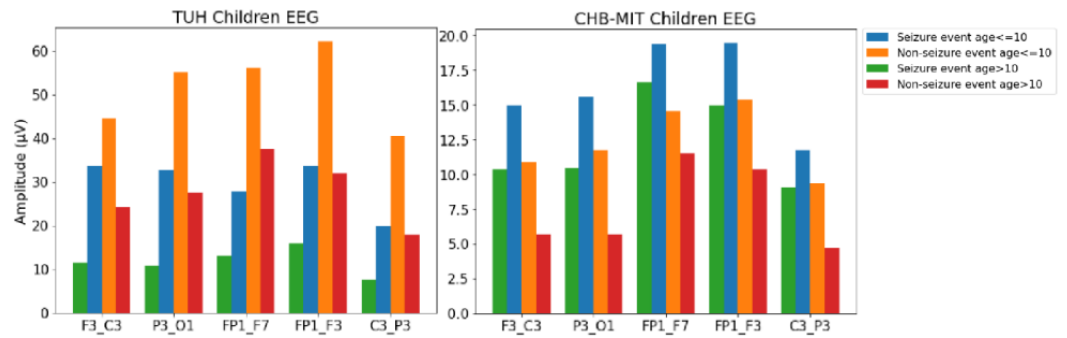


Figure 7. Comparison of mean amplitude between seizure events and non-seizure events for children with age > 10 and age ≤ 10 across five selected channels on the TUH pediatric and adolescent EEG and CHB-MIT pediatric and adolescent EEG.

4.3. Previous Work on Seizure Detection Using TUH and CHB-MIT EEGs

Research on automatic seizure detection, particularly when trained and tested on different databases, has been limited. However, several studies have explored the application of various algorithms for automated seizure detection in TUH EEG or CHB-MIT EEG datasets. Table 3 summarizes previous seizure detection methods applied to the TUH EEG and CHB-MIT EEG datasets.

Table 3. Seizure detection methods for TUH and CHB-MIT EEGs.

	Reference	Method	Sensitivity	Specificity	Accuracy
TUH	[8]	CNN + LSTM	30%	-	-
	[13]	Convolutional LSTM	30%	-	-
	[9]	2D CNN	39.2%	90.4%	-
	[10]	CNN + MLP	31.58%		
	[11]	WaveNet + LSTM			88.76%
	[39]	CNN			86.59%
	[15]	Random forest	67.5%	71.1%	-
CHB-MIT	[40]	XGBoost	20%	-	-
	[41]	KNN	88%	88%	93%
	[42]	VGG16	85.94%	-	85.41%
	[43]	SVM	90.62%	99.32%	-
	[44]	Bi-LSTM	93.61%	91.85%	-
	[45]	Random forest	93.60%	93.37%	-

4.4. Performance on TUH and CHB-MIT EEG

Table 4 presents the outcomes of the four seizure detection models based on LightGBM, evaluated on the training set, validation set, and independent test set. Notably, Model 2 exhibits the worst performance on the independent test set in comparison to the other models. Model 4 excels in performance on the validation set, while Model 3 demonstrates the best performance on the independent test set.

Table 4. Performance of the LightGBM-based seizure detection methods on the training, validation and independent test set (TUH children and CHB-MIT pediatric and adolescent EEG).

	Dataset	Database	Sensitivity (%)	Specificity (%)	Accuracy (%)	Balanced Accuracy (%)
Model 1	Train	TUH Children	95.18	96.85	96.68	96.01
	Validation	TUH Children	94.97	96.47	96.32	95.72
	Test	TUH Children	73.15	95.72	98.68	86.15
	Test	CHB-MIT	58.82	62.15	62.09	60.48
Model 2	Train	TUH Children	95.55	96.93	96.79	96.24
	Validation	TUH Children	94.89	96.53	96.37	95.71
	Test	TUH Children	75.07	99.25	98.82	87.16
	Test	CHB-MIT	62.31	57.56	57.65	59.93

Table 4. Cont.

	Dataset	Database	Sensitivity (%)	Specificity (%)	Accuracy (%)	Balanced Accuracy (%)
Model 3	Train	TUH Children	95.51	96.91	96.77	96.21
	Validation	TUH Children	95.23	96.57	96.44	95.90
	Test	TUH Children	74.28	99.40	98.95	86.84
	Test	CHB-MIT	59.08	64.92	64.82	62.00
Model 4	Train	TUH Children	95.57	97.05	96.90	96.31
	Validation	TUH Children	95.20	96.69	96.54	95.95
	Test	TUH Children	73.50	99.39	98.93	86.45
	Test	CHB-MIT	59.58	62.81	62.76	61.20

5. Discussion

Many existing seizure detection methods have been primarily tailored to adult EEG data [10,12,13]. However, the application of these methods to pediatric and adolescent EEG data are considerably limited. Research has unequivocally demonstrated that the adaptation of adult-based methodologies to children is not a viable solution [15]. Consequently, there exists a pressing need for the development of seizure detection methods specifically designed for the pediatric and adolescent population [15]. Moreover, research into automated seizure detection, especially when trained and tested on diverse databases, has been relatively restricted. Several studies have investigated the use of different algorithms for automated seizure detection in TUH EEG or CHB-MIT EEG datasets (refer to Table 3). However, these studies primarily focused on training and testing on the same database, leaving the performance of external databases largely unexplored.

These gaps were addressed by introducing novel automatic seizure detection methods explicitly tailored to pediatric and adolescent EEG data. To ensure the robustness of the method, a five-fold cross-validation approach was employed. Our method achieved an average sensitivity of 97.52%, average specificity of 96.76%, average accuracy of 97.14%, and average balanced accuracy of 97.14% on the training set. Moreover, the pediatric and adolescent datasets were partitioned into distinct training and testing sets, guaranteeing the independence of the test data. The method achieved an accuracy rate of 98.95% on the TUH test set. Additionally, the method was subjected to rigorous evaluation on an external test set, the CHB-MIT EEGs, where it exhibited an accuracy of 64.82%.

Furthermore, it is well-established that brain events in EEG data evolve with age [14]. Previous research has illuminated disparities in rhythm activities between male and female children [16]. Thus, the potential impacts of age and sex were explored on the detection of seizures in pediatric and adolescent EEG. Four distinct models were crafted for seizure detection in pediatric and adolescent EEG.

Four distinct LightGBM-based models were developed for seizure detection in pediatric and adolescent EEG data. The baseline model (Model 1) using 20 features from time and frequency domains served as the initial benchmark. These 20 features have been commonly employed in previous studies focusing on EEG analysis [46,47]. Model 2's addition of sex as a feature to assess the importance of sex in pediatric seizure detection, exhibited a slight improvement of 0.14% in accuracy on the TUH test set. However, its adverse impact on the CHB-MIT EEG data, resulting in a decrease of approximately 5%, prompts scrutiny into the complex interplay of sex as a predictive feature in different datasets. Model 3, integrating age group as a feature, demonstrated improvements in accuracy on both the TUH test set and the CHB-MIT EEG test set compared to the baseline model. The decision to categorize age into two groups, 0–10 years and 10–20 years, was based on existing literature citing distinct neurological developmental stages between pre-adolescents and adolescents [48,49]. Model 4, extending from Model 3 by incorporating sex as an additional feature, paradoxically resulted in reduced accuracy on the independent test set. This observation emphasizes the intricate relationship between demographic variables and EEG features in seizure detection. The uncertainty surrounding the impact of sex in the models underscores the necessity for a deeper investigation into its role and potential correlations

with other variables present in the dataset. Our findings strongly indicate age group as a key feature in EEG-based seizure detection, superseding other demographic variables in its influence. Figure 4 illustrates the pronounced significance of age as a contributing factor in the seizure detection process, showcasing its prominence over sex as observed in the model outcomes.

Our previous study [15] trained models using the TUH adult EEG data and tested them on the CHB-MIT EEG data. This approach was not successful, with a sensitivity of 91.2%, specificity of 10.3%, and an accuracy of only 10.5% and a balanced accuracy of 50.8% on the CHB-MIT EEG dataset. It is apparent that our previous method achieved a high sensitivity, but suffered from low specificity and accuracy. This suggests that the previous method exhibited a high true positive rate (TP), low false negative rate (FN), and true negatives (TN). Essentially, the method tended to classify nearly every event as a seizure event, leading to subpar performance. This could be attributed to the resemblance of features between non-seizure events in pediatrics and seizure events in adults, thereby adversely impacting performance. Therefore, there is a need to develop a pediatric-specific seizure detection method. However, in this work, training on TUH pediatric and adolescent EEG data and testing on CHB-MIT EEG data, yielded significantly improved results, achieving an accuracy of 64.82% and a balanced accuracy of 62.00% on the CHB-MIT EEG dataset. These findings strongly indicate that age-related differences play an important role in EEG patterns and their interpretation.

Due to its simplicity and ease of implementation, the Teager–Kaiser Energy Operator (TKEO) has proven to be a valuable tool for detecting changes in signal properties in various applications, as demonstrated in prior research [46]. The investigation has further underscored the significance of TKEO as a feature for the identification of seizure events, as depicted in Figure 4. Furthermore, Figure 5 presents a comprehensive comparison of TKEO values between seizure events and non-seizure events across five specific channels in both the TUH pediatric and adolescent EEG and CHB-MIT pediatric and adolescent EEG datasets. In the case of the TUH EEG data, it is evident that most of the TKEO values for seizure events are significantly lower than those for non-seizure events, particularly on channels P3-O1, FP1-F7, and C3-P3. A similar trend is observed in the CHB-MIT EEG data, where TKEO values for seizure events are lower than those for non-seizure events on channels F3-C3, P3-O1, FP1-F7, and FP1-F3. These findings underscore the marked distinctions in TKEO values between seizure and non-seizure events across a range of channels.

An analysis of mean amplitude differences between seizure and non-seizure events was conducted, with a specific focus on sex, across five designated channels within the TUH pediatric and adolescent EEG and CHB-MIT pediatric and adolescent EEG datasets. The findings, as depicted in Figure 6, reveal distinct patterns. For the CHB-MIT EEGs, it is evident that the mean amplitude during seizure events is higher than during non-seizure events for both males and females across the selected five channels. However, a noteworthy divergence is observed in the case of TUH male EEGs, where the mean amplitude during non-seizure events surpasses that of seizure events.

Gender disparities in epilepsy are prevalent and extend across a spectrum of epilepsy syndromes. The magnitude of these differences fluctuates among distinct seizure disorders, with notable impacts from age-related factors. Notably, women exhibit a higher prevalence of diagnoses in idiopathic generalized epilepsies compared to men [50]. Carlson et al. [51] revealed significant gender disparities in the occurrence of atonic seizures, which were more prevalent in males with generalized epilepsy, as well as in autonomic, visual, and psychic symptoms associated with nonacquired focal epilepsy, which were more common in females. Additionally, research [52] has highlighted distinct studies linking temporal lobe seizure characteristics with age. Similarly, investigation [53] emphasized the age dependency of EEG, suggesting the need to examine the impact of age on seizures and non-seizure events.

Despite the growing interest in sex and age differences in disease presentations and treatment responses, data are scarce on sex and age analysis in seizures and non-seizures. We

incorporate age and sex as features to develop the method and analyze the features in seizure and non-seizure events between age and sex. This study found that among female EEGs, the mean amplitude during seizure events exceeds that of non-seizure events on specific channels (F3-C3, P3-O1, and C3-P3), while it is lower on other channels (FP1-F7 and FP1-F3). Interestingly, Figure 6 reveals that the mean amplitude during seizure events is consistently higher for females compared to males in both TUH and CHB-MIT EEGs. Additionally, the mean amplitude during non-seizure events tends to be lower for females compared to males in both datasets. Nevertheless, the analysis undertaken earlier revealed certain disparities in the amplitudes observed between males and females during both seizure and non-seizure events in the five selected channels within the two datasets. As a result, it remains challenging to conclusively determine the impact of sex on the efficacy of seizure detection.

A comparison of mean amplitude between seizure and non-seizure events in children aged over 10 and those aged 10 or younger was conducted, considering five specific channels within the TUH pediatric and adolescent EEG and CHB-MIT pediatric and adolescent EEG datasets. As illustrated in Figure 7, significant trends emerge. For TUH EEGs, it is evident that the mean amplitude during non-seizure events surpasses that of seizure events in both age groups (1. aged over 10, and 2. those aged 10 or younger) across the selected five channels. Conversely, in CHB-MIT EEGs, an intriguing finding is that the mean amplitude during non-seizure events is lower than during seizure events for both age groups (1. aged over 10, and 2. those aged 10 or younger) in the selected five channels.

It is noteworthy that, across both the TUH and CHB-MIT EEG datasets, the mean amplitude of non-seizure events within the younger age group is consistently higher than that of the older age group in the selected five channels. Additionally, the mean amplitude of seizure events within children aged 10 or younger also consistently exceeds that of children aged over 10 years old in the same channels within both datasets.

To further assess the potential differences in seizure events between children aged 10 or younger and those aged over 10 years, *t*-tests were conducted on the seizure events within the selected five channels in pediatric and adolescent EEG data. For the CHB-MIT EEGs, the results (p -value ≥ 0.05) indicated that there was no significant difference between the seizure events in the two age groups across various channels. This lack of significance might be attributed to differences in sample size, as the CHB-MIT EEG dataset had only 22 patients. Consequently, the disparities may not have been readily apparent.

In the case of the TUH EEGs with a larger sample size ($N = 184$), the results (p -value < 0.05) demonstrated a significant difference between the seizure events in the two age groups across different channels. This comprehensive analysis underscores the evident impact of age on the amplitude differences in epilepsy, particularly within the TUH pediatric and adolescent dataset, highlighting the evident impact of age on the process of seizure detection. Consequently, it is highly recommended to include age as a pertinent feature when devising automated methods for seizure detection.

The limitation of this study lies in its performance on the CHB-MIT EEG dataset, where the accuracy was 64.82%. This discrepancy may be attributed to the distinct EEG recording methods employed by the TUH EEG and CHB-MIT EEG datasets, potentially resulting in differences in EEG patterns that affect the overall performance. Furthermore, the TUH EEG dataset encompasses Absence Seizures, Complex Partial Seizures, Focal Non-Specific Seizures, Generalized Seizures, Tonic-Clonic Seizures, Tonic Seizures, Simple Partial Seizures, and Myoclonic Seizures. In contrast, the CHB-MIT EEG dataset includes clonic Seizures, atonic Seizures, and tonic Seizures. The varying types of seizures present in each dataset might contribute to the lower performance observed in the CHB-MIT EEG compared to the TUH pediatric and adolescent EEG. Another limitation is that the classifier incorporates age by implementing a threshold on the age range (>10 and ≤ 10), rather than using the original age values. Such methodologies might not be effective for datasets with limited age ranges.

The dataset's size and diversity might not fully represent the complexity and variability of pediatric and adolescent EEG data in clinical scenarios. This limitation could affect the model's generalizability to diverse patient populations or specific clinical conditions not extensively

covered in the dataset. Additionally, while age and sex were incorporated as features, other potentially influential factors may exist, such as varying EEG acquisition protocols which were not comprehensively addressed. The absence of these factors could limit the model's robustness and performance in clinical settings where such variations are prevalent.

It is worth noting that the TUH EEG dataset encompasses a broader spectrum of seizure types, including focal non-specific seizures, generalized seizures, tonic-clonic seizures, and tonic seizures [33], whereas the CHB-MIT EEG dataset primarily consists of clonic, tonic, and atonic seizures [54]. Given the variations in seizure patterns and rhythm activities associated with different seizure types, it is plausible that this diversity contributed to the lower accuracy observed on the CHB-MIT EEG dataset. Nonetheless, it is important to highlight that this study was conducted across different subjects and databases, achieving a respectable level of performance. This study is dedicated to examining the influence of age and sex on seizure detection in pediatric and adolescent EEG. Consequently, the specific seizure type was not taken into account. Nevertheless, acknowledging the significant impact that seizure type may have on seizure detection. Future work will investigate the impact of seizure type by using uniform seizure types in both the TUH and CHB-MIT EEG datasets. This approach will allow us to explore whether the specific type of seizure has a discernible influence on the performance of the models.

6. Conclusions

A seizure detection method was developed using LightGBM applied to pediatric and adolescent EEG recordings. To ensure the independence of test sets, the children were partitioned into distinct training and testing sets, resulting in the highest accuracy of 98.95% on the TUH test set. Furthermore, an evaluation of the method using an external test set (CHB-MIT EEGs) was conducted, reaching a peak accuracy of 64.82%. Additionally, the impact of age and sex on seizure detection was explored, revealing that age is a critical factor in this process. Our findings hold significant promise for enhancing the speed, reliability, and repeatability of seizure analysis in pediatric and adolescent EEGs, thereby contributing to advancements in research and clinical applications.

Author Contributions: Conceptualization, L.W. and C.M.; Investigation, L.W.; Methodology, L.W.; Software, L.W.; Supervision, C.M.; Validation, L.W.; Visualization, L.W.; Writing—original draft, L.W.; Writing—review and editing, L.W. and C.M. All authors have read and agreed to the published version of the manuscript.

Funding: This project has received funding from the European Union's Horizon 2020 Research and Innovation Programme under the NeuroInsight Marie Skłodowska-Curie grant agreement No. 101034252. This publication has emanated from research supported in part by a research grant from Science Foundation Ireland (SFI) under Grant Number 21/RC/10294 and co-funded under the European Regional Development Fund and by FutureNeuro industry partners. We acknowledge the Research IT HPC Service at University College Dublin for providing computational facilities and support that contributed to the research results reported in this paper.

Institutional Review Board Statement: Not applicable.

Informed Consent Statement: Not applicable.

Data Availability Statement: TUH EEG data collected by Temple University Hospital, which can be used for both research and commercialization purposes. The data could be downloaded through https://isip.piconepress.com/projects/tuh_eeg/ (accessed on 29 January 2024). CHB-MIT EEG collected at the Children's Hospital Boston, consists of EEG recordings from pediatric subjects with intractable seizures. The data could be downloaded through <https://physionet.org/content/chbmit/1.0.0/> (accessed on 29 January 2024).

Conflicts of Interest: The authors declare no conflicts of interest.

References

1. Thijs, R.D.; Surges, R.; O'Brien, T.J.; Sander, J.W. Epilepsy in adults. *Lancet* **2019**, *393*, 689–701. [CrossRef]

2. Guerrini, R. Epilepsy in children. *Lancet* **2006**, *367*, 499–524. [[CrossRef](#)]
3. Fountain, N.B.; Freeman, J.M. EEG is an essential clinical tool: Pro and con. *Epilepsia* **2006**, *47*, 23–25. [[CrossRef](#)]
4. Bohr, A.; Memarzadeh, K. The rise of artificial intelligence in healthcare applications. In *Artificial Intelligence in Healthcare*; Elsevier: Copenhagen, Denmark, 2020; pp. 25–60.
5. Rajpurkar, P.; Irvin, J.; Ball, R.L.; Zhu, K.; Yang, B.; Mehta, H.; Duan, T.; Ding, D.; Bagul, A.; Langlotz, C.P.; et al. Deep learning for chest radiograph diagnosis: A retrospective comparison of the CheXNeXt algorithm to practicing radiologists. *PLoS Med.* **2018**, *15*, e1002686. [[CrossRef](#)]
6. Hannun, A.Y.; Rajpurkar, P.; Haghpanahi, M.; Tison, G.H.; Bourn, C.; Turakhia, M.P.; Ng, A.Y. Cardiologist-level arrhythmia detection and classification in ambulatory electrocardiograms using a deep neural network. *Nat. Med.* **2019**, *25*, 65–69. [[CrossRef](#)]
7. Rajpurkar, P.; Chen, E.; Banerjee, O.; Topol, E.J. AI in health and medicine. *Nat. Med.* **2022**, *28*, 31–38. [[CrossRef](#)]
8. Golmohammadi, M.; Ziyabari, S.; Shah, V.; Obeid, I.; Picone, J. Deep architectures for spatio-temporal modeling: Automated seizure detection in scalp EEGs. In Proceedings of the 2018 17th IEEE International Conference on Machine Learning and Applications (ICMLA), Orlando, FL, USA, 17–20 December 2018; pp. 745–750.
9. Shah, V.; Golmohammadi, M.; Ziyabari, S.; Von Weltin, E.; Obeid, I.; Picone, J. Optimizing channel selection for seizure detection. In Proceedings of the 2017 IEEE Signal Processing in Medicine and Biology Symposium (SPMB), Philadelphia, PA, USA, 2 December 2017; pp. 1–5.
10. Ziyabari, S.; Shah, V.; Golmohammadi, M.; Obeid, I.; Picone, J. Objective evaluation metrics for automatic classification of EEG events. *arXiv* **2017**, arXiv:1712.10107.
11. Albaqami, H.; Hassan, G.M.; Datta, A. Automatic detection of abnormal eeg signals using wavenet and lstm. *Sensors* **2023**, *23*, 5960. [[CrossRef](#)]
12. He, K.; Zhang, X.; Ren, S.; Sun, J. Delving deep into rectifiers: Surpassing human-level performance on imagenet classification. In Proceedings of the IEEE International Conference on Computer Vision, Santiago, Chile, 7–13 December 2015; pp. 1026–1034.
13. Golmohammadi, M.; Ziyabari, S.; Shah, V.; Von Weltin, E.; Campbell, C.; Obeid, I.; Picone, J. Gated recurrent networks for seizure detection. In Proceedings of the 2017 IEEE Signal Processing in Medicine and Biology Symposium (SPMB), Philadelphia, PA, USA, 2 December 2017; pp. 1–5.
14. Vysata, O.; Kukal, J.; Prochazka, A.; Pazdera, L.; Simko, J.; Valis, M. Age-related changes in EEG coherence. *Neurol. Neurochir. Pol.* **2014**, *48*, 35–38. [[CrossRef](#)]
15. Wei, L.; Mooney, C. Investigating the Need for Pediatric-Specific Machine Learning Approaches for Seizure Detection in EEG. In Proceedings of the 2023 11th International Conference on Bioinformatics and Computational Biology (ICBCB), Hangzhou, China, 21–23 April 2023; pp. 57–63.
16. Wei, L.; McHugh, J.C.; Mooney, C. A Machine Learning Approach for Sex and Age Classification of Paediatric EEGs. In Proceedings of the 2023 45th Annual International Conference of the IEEE Engineering in Medicine & Biology Society (EMBC), Sydney, Australia, 24–27 July 2023; pp. 1–4.
17. Bresnahan, S.M.; Anderson, J.W.; Barry, R.J. Age-related changes in quantitative EEG in attention-deficit/hyperactivity disorder. *Biol. Psychiatry* **1999**, *46*, 1690–1697. [[CrossRef](#)]
18. Duffy, F.H.; Albert, M.S.; McAnulty, G.; Garvey, A.J. Age-related differences in brain electrical activity of healthy subjects. *Ann. Neurol. Off. J. Am. Neurol. Assoc. Child Neurol. Soc.* **1984**, *16*, 430–438. [[CrossRef](#)]
19. Pierce, T.W.; Watson, T.D.; King, J.S.; Kelly, S.P.; Pribram, K.H. Age differences in factor analysis of EEG. *Brain Topogr.* **2003**, *16*, 19–27. [[CrossRef](#)]
20. Marciani, M.G.; Maschio, M.; Spanedda, F.; Caltagirone, C.; Gigli, G.; Bernardi, G. Quantitative EEG evaluation in normal elderly subjects during mental processes: Age-related changes. *Int. J. Neurosci.* **1994**, *76*, 131–140. [[CrossRef](#)]
21. Klass, D.W.; Brenner, R.P. Electroencephalography of the elderly. *J. Clin. Neurophysiol.* **1995**, *12*, 116–131. [[CrossRef](#)]
22. Hartikainen, P.; Soininen, H.; Partanen, J.; Helkala, E.; Riekkinen, P. Aging and spectral analysis of EEG in normal subjects: A link to memory and CSF AChE. *Acta Neurol. Scand.* **1992**, *86*, 148–155. [[CrossRef](#)]
23. Gasser, T.; Verleger, R.; Bächer, P.; Sroka, L. Development of the EEG of school-age children and adolescents. I. Analysis of band power. *Electroencephalogr. Clin. Neurophysiol.* **1988**, *69*, 91–99. [[CrossRef](#)]
24. Clarke, A.R.; Barry, R.J.; McCarthy, R.; Selikowitz, M. Age and sex effects in the EEG: Development of the normal child. *Clin. Neurophysiol.* **2001**, *112*, 806–814. [[CrossRef](#)]
25. Petersén, I.; Eeg-Olofsson, O. The development of the electroencephalogram in normal children from the age of 1 through 15 years—non-paroxysmal activity. *Neuropädiatrie* **1971**, *2*, 247–304. [[CrossRef](#)]
26. Matousek, M. Frequency analysis of the EEG in normal children and adolescents. In *Automation of Clinical Electroencephalography*; Raven Press: New York, NY, USA, 1973; pp. 75–102.
27. Cohn, N.; Kircher, J.; Emmerson, R.; Dustman, R. Pattern reversal evoked potentials: Age, sex and hemispheric asymmetry. *Electroencephalogr. Clin. Neurophysiol. Potentials Sect.* **1985**, *62*, 399–405. [[CrossRef](#)]
28. Matthis, P.; Scheffner, D.; Benninger, C.; Lipinski, C.; Stolzis, L. Changes in the background activity of the electroencephalogram according to age. *Electroencephalogr. Clin. Neurophysiol.* **1980**, *49*, 626–635. [[CrossRef](#)]
29. Zeng, H.; Yang, C.; Zhang, H.; Wu, Z.; Zhang, J.; Dai, G.; Babiloni, F.; Kong, W. A lightGBM-based EEG analysis method for driver mental states classification. *Comput. Intell. Neurosci.* **2019**, *2019*, 3761203. [[CrossRef](#)]
30. Chatterjee, S.; Byun, Y.C. EEG-based emotion classification using stacking ensemble approach. *Sensors* **2022**, *22*, 8550. [[CrossRef](#)]

31. Aggarwal, S.; Aggarwal, L.; Rihal, M.S.; Aggarwal, S. EEG based participant independent emotion classification using gradient boosting machines. In Proceedings of the 2018 IEEE 8th International Advance Computing Conference (IACC), Greater Noida, India, 14–15 December 2018; pp. 266–271.
32. Harati, A.; Lopez, S.; Obeid, I.; Picone, J.; Jacobson, M.; Tobochnik, S. The TUH EEG CORPUS: A big data resource for automated EEG interpretation. In Proceedings of the 2014 IEEE Signal Processing in Medicine and Biology Symposium (SPMB), Philadelphia, PA, USA, 13 December 2014; pp. 1–5.
33. Statsenko, Y.; Babushkin, V.; Talako, T.; Kurbatova, T.; Smetanina, D.; Simiyu, G.L.; Habuza, T.; Ismail, F.; Almansoori, T.M.; Gorkom, K.N.V.; et al. Automatic Detection and Classification of Epileptic Seizures from EEG Data: Finding Optimal Acquisition Settings and Testing Interpretable Machine Learning Approach. *Biomedicines* **2023**, *11*, 2370. [CrossRef]
34. Shoeb, A.H. Application of Machine Learning to Epileptic Seizure Onset Detection and Treatment. Ph.D. Thesis, Massachusetts Institute of Technology, Cambridge, MA, USA, 2009.
35. Siuly, S.; Li, Y.; Zhang, Y. EEG signal analysis and classification. *IEEE Trans. Neural Syst. Rehabil. Eng.* **2016**, *11*, 141–144.
36. Chawla, N.V.; Bowyer, K.W.; Hall, L.O.; Kegelmeyer, W.P. SMOTE: Synthetic minority over-sampling technique. *J. Artif. Intell. Res.* **2002**, *16*, 321–357. [CrossRef]
37. Ke, G.; Meng, Q.; Finley, T.; Wang, T.; Chen, W.; Ma, W.; Ye, Q.; Liu, T.Y. Lightgbm: A highly efficient gradient boosting decision tree. *Adv. Neural Inf. Process. Syst.* **2017**, *30*, 3149–3157.
38. Li, K.; Xu, H.; Liu, X. Analysis and visualization of accidents severity based on LightGBM-TPE. *Chaos Solitons Fractals* **2022**, *157*, 111987. [CrossRef]
39. Kiessner, A.K.; Schirrmester, R.T.; Gemein, L.A.; Boedecker, J.; Ball, T. An extended clinical EEG dataset with 15,300 automatically labelled recordings for pathology decoding. *NeuroImage Clin.* **2023**, *39*, 103482. [CrossRef]
40. Wei, L.; Mooney, C. Epileptic seizure detection in clinical EEGs using an XGBoost-based method. In Proceedings of the 2020 IEEE Signal Processing in Medicine and Biology Symposium (SPMB), Philadelphia, PA, USA, 5 December 2020; pp. 1–6.
41. Fergus, P.; Hussain, A.; Hignett, D.; Al-Jumeily, D.; Abdel-Aziz, K.; Hamdan, H. A machine learning system for automated whole-brain seizure detection. *Appl. Comput. Inform.* **2016**, *12*, 70–89. [CrossRef]
42. Wei, L.; Mooney, C. Transfer Learning-based Seizure Detection on Multiple Channels of Paediatric EEGs. In Proceedings of the 2023 45th Annual International Conference of the IEEE Engineering in Medicine & Biology Society (EMBC), Sydney, Australia, 24–27 July 2023; p. 1–4.
43. Zabih, M.; Kiranyaz, S.; Ince, T.; Gabbouj, M. Patient-specific epileptic seizure detection in long-term EEG recording in paediatric patients with intractable seizures. In Proceedings of the IET Intelligent Signal Processing Conference 2013 (ISP 2013), London, UK, 2–3 December 2013.
44. Hu, X.; Yuan, S.; Xu, F.; Leng, Y.; Yuan, K.; Yuan, Q. Scalp EEG classification using deep Bi-LSTM network for seizure detection. *Comput. Biol. Med.* **2020**, *124*, 103919. [CrossRef]
45. Sopic, D.; Aminifar, A.; Atienza, D. e-glass: A wearable system for real-time detection of epileptic seizures. In Proceedings of the 2018 IEEE International Symposium on Circuits and Systems (ISCAS), Florence, Italy, 27–30 May 2018; pp. 1–5.
46. Wei, L.; Boutouil, H.; Gerbatin, R.R.; Mamad, O.; Heiland, M.; Reschke, C.R.; Del Gallo, F.; Fabene, P.F.; Henshall, D.C.; Lowery, M.; et al. Detection of spontaneous seizures in EEGs in multiple experimental mouse models of epilepsy. *J. Neural Eng.* **2021**, *18*, 056060. [CrossRef]
47. Wei, L.; Mooney, C. Investigating the Need for Pediatric-Specific Automatic Seizure Detection. In Proceedings of the 2022 IEEE Signal Processing in Medicine and Biology Symposium (SPMB), Philadelphia, PA, USA, 3 December 2022; pp. 1–3.
48. World Health Organization. Adolescent Health. Available online: https://www.who.int/health-topics/adolescent-health#tab=tab_1 (accessed on 12 December 2023).
49. Kałwak, K.; Porwolik, J.; Mielcarek, M.; Gorczyńska, E.; Owoc-Lempach, J.; Ussowicz, M.; Dyla, A.; Musiał, J.; Paździor, D.; Turkiewicz, D.; et al. Higher CD34+ and CD3+ cell doses in the graft promote long-term survival, and have no impact on the incidence of severe acute or chronic graft-versus-host disease after in vivo T cell-depleted unrelated donor hematopoietic stem cell transplantation in children. *Biol. Blood Marrow Transplant.* **2010**, *16*, 1388–1401.
50. Reddy, D.S.; Thompson, W.; Calderara, G. Molecular mechanisms of sex differences in epilepsy and seizure susceptibility in chemical, genetic and acquired epileptogenesis. *Neurosci. Lett.* **2021**, *750*, 135753. [CrossRef]
51. Carlson, C.; Dugan, P.; Kirsch, H.E.; Friedman, D.; EPGP Investigators. Sex differences in seizure types and symptoms. *Epilepsy Behav.* **2014**, *41*, 103–108. [CrossRef]
52. Fogarasi, A.; Tuxhorn, I.; Janszky, J.; Janszky, I.; Rásonyi, G.; Kelemen, A.; Halász, P. Age-dependent seizure semiology in temporal lobe epilepsy. *Epilepsia* **2007**, *48*, 1697–1702. [CrossRef]
53. Greene, B.R.; Faul, S.; Marnane, W.; Lightbody, G.; Korotchikova, I.; Boylan, G.B. A comparison of quantitative EEG features for neonatal seizure detection. *Clin. Neurophysiol.* **2008**, *119*, 1248–1261. [CrossRef]
54. Alharthi, M.K.; Moria, K.M.; Alghazzawi, D.M.; Tayeb, H.O. Epileptic Disorder Detection of Seizures Using EEG Signals. *Sensors* **2022**, *22*, 6592. [CrossRef]

Disclaimer/Publisher’s Note: The statements, opinions and data contained in all publications are solely those of the individual author(s) and contributor(s) and not of MDPI and/or the editor(s). MDPI and/or the editor(s) disclaim responsibility for any injury to people or property resulting from any ideas, methods, instructions or products referred to in the content.